Arabian Journal of Chemistry (2015) xxx, xxx–xxx

King Saud University

Arabian Journal of Chemistry

www.ksu.edu.sa
www.sciencedirect.com

ORIGINAL ARTICLE

Electrochemistry of myoglobin on graphene–SnO_2 nanocomposite modified electrode and its electrocatalysis

Wencheng Wang [a], Lifeng Dong [b,c,*], Shixing Gong [b], Ying Deng [b], Jianhua Yu [b], Hongzhou Dong [b], Tianyou Wang [a], Wei Sun [a,*]

[a] *College of Chemistry and Chemical Engineering, Hainan Normal University, Haikou 571158, PR China*
[b] *College of Materials Science and Engineering, Qingdao University of Science and Technology, Qingdao 266042, PR China*
[c] *Department of Physics, Hamline University, St. Paul, MN 55104, USA*

Received 7 May 2015; accepted 16 September 2015

KEYWORDS

Carbon ionic liquid electrode;
Direct electrochemistry;
Graphene;
Myoglobin;
SnO_2

Abstract In this paper direct electrochemistry and electrocatalysis of myoglobin (Mb) immobilized on a graphene (GR)–SnO_2 nanocomposite modified carbon ionic liquid electrode was reported. GR–SnO_2 nanocomposite was synthesized by a simple solution method and further characterized by TEM and SEM, which exhibited large surface area beneficial for Mb immobilization. Spectroscopic results indicated Mb retained its native structure without denaturation after mixed with nanocomposite. Electrochemical investigation showed that a pair of well-defined redox peaks appeared on cyclic voltammogram, indicating that direct electron transfer of Mb with the underlying electrode was realized. The results could be attributed to the presence of GR–SnO_2 nanocomposite that could enhance the electron transfer between the protein and the electrode. The Mb modified electrode exhibited good stability and catalytic activity to the electroreduction of $NaNO_2$ in the concentration range from 0.2 to 350.0 μmol L^{-1} with wider dynamic range and lower detection limit. Therefore the fabricated electrode has the potential application in the third-generation electrochemical biosensor.

* Corresponding authors at: College of Materials Science and Engineering, Qingdao University of Science and Technology, Qingdao 266042, PR China. Tel.: +86 532 84022869 (L. Dong). Tel.: +86 898 31381637 (W. Sun).
E-mail addresses: donglifeng@qust.edu.cn (L. Dong), swyy26@hotmail.com (W. Sun).
Peer review under responsibility of King Saud University.

Production and hosting by Elsevier

1. Introduction

As a flat monolayer of carbon atoms in a closely packed honeycomb two-dimensional lattice, graphene (GR) has attracted immense attentions in recent years (Geim and Novoselov, 2007; Li et al., 2008). GR exhibits many unique properties, such as high surface area, remarkable thermal conductivity, excellent electronic conductivity and good biocompatibility, which render GR various applications in different fields such

http://dx.doi.org/10.1016/j.arabjc.2015.09.007
1878-5352

Please cite this article in press as: Wang, W. et al., Electrochemistry of myoglobin on graphene–SnO_2 nanocomposite modified electrode and its electrocatalysis. Arabian Journal of Chemistry (2015), http://dx.doi.org/10.1016/j.arabjc.2015.09.007

as sensors, fuel cells, energy conversion and so on (Brownson et al., 2012; Pumera, 2010). The synthesis and applications of GR and its related composites in the field of electrochemistry and electrochemical sensors have also been reviewed (Shao et al., 2010; Chen et al., 2010). Due to the interlayer structure of GR nanosheets with lattice defect and surface functional groups, different kinds of nanomaterials can be anchored on the GR surface to get their nanocomposite, which exhibit synergistic effects with wide applications (Wang et al., 2012; Singh et al., 2011).

As an n-type wide band gap semiconductor, tin dioxide (SnO_2) has been extensively used in the fields of gas sensors, optoelectronic devices, supercapacitors, lithium-ion batteries and photocatalyst due to its diverse optical and electrical properties, high theoretical capacity, low cost and low toxicity (Idota et al., 1997; Sahm et al., 2007). Many reports have been published for the synthesis of SnO_2 nanomaterials with various geometrical morphologies by different methods (Zhu et al., 2000; Krishnakumar et al., 2008; Yang and Wang, 2007). Recently GR and SnO_2 nanocomposites have been synthesized and used in the field of electrochemistry. The combinations of GR and SnO_2 nanomaterials exhibit synergistic effects including improved mechanical strength, electronic conductivity and excellent electrochemical properties. Yao et al. developed an in situ chemical synthesis approach for GR–SnO_2 nanocomposite, which was used as anode materials for lithium-ion batteries (Yao et al., 2009). Li et al. prepared SnO_2 nanocrystals/GR composites and investigated the lithium storage ability (Li et al., 2010). Lu et al. investigated the electrochemical behaviors of GR–SnO_2 composite film for supercapacitors (Lu et al., 2010). Huang et al. proposed a one-step solvothermal method for the synthesis of GR–SnO_2 nanocomposite and investigated its application as the anode material for lithium-ion batteries (Huang et al., 2011). Ding et al. demonstrated a hydrothermal method to grow SnO_2 nanosheets directly on GR sheets, which exhibited enhanced lithium storage properties with high reversible capacities and good cycling performances (Ding et al., 2011). Wang et al. developed a simple solution-based synthesis route for GR–SnO_2 composite used as the high stability electrode for lithium ion batteries (Wang et al., 2011). Sun et al. applied a GR–SnO_2 nanocomposite modified electrode for the electrochemical detection of dopamine (Sun et al., 2013). Lian et al. prepared a porous SnO_2@C/GR nanocomposite as a superior anode material for lithium ion batteries (Lian et al., 2014). However, there are seldom reports about the application of GR–SnO_2 nanocomposite in the protein electrochemistry.

Direct electrochemistry of redox proteins with the substrate electrodes has aroused great interests in recent years. The results can be used for the electrochemical mechanism investigation, and the fabrication of biosensors and biodevices (Armstrong et al., 1988; Rusling, 1998). The third-generation electrochemical enzyme sensor is based on the direct electron transfer reactions between the prosthetic group of the enzyme and the electrode, which is more efficient in electrical communication than the first-generation and second-generation biosensors that use natural secondary substrates and artificial redox mediators (Wang, 2006). The third-generation biosensors exhibit the advantages such as superior selectivity without the interfering reaction, and the possibility of modulating the desired properties of sensor with protein modification or novel interfacial technologies (Gorton et al., 1999).

With the development of nanotechnology, various nanomaterials have been used for the preparation of chemically modified electrodes, which can facilitate the electron transfer between proteins and electrodes. The presence of nanomaterials on the electrode surface can increase the interfacial area, construct an electron transfer route and remain the structure of the redox proteins (Mani et al., 2012). Due to the specific properties of GR and GR-based nanocomposites such as high electronic conductivity, large surface area and good biocompatibility, GR modified electrodes have been used in the field of protein electrochemistry (Gan and Hu, 2011). In this paper GR–SnO_2 nanocomposite was synthesized by a simple solution method based on reduction of graphene oxide (GO) with Sn^{2+} ion. The GR–SnO_2 nanocomposite can be generated by using the strong reductive capability of Sn^{2+} with the GO reduction and Sn^{2+} oxidation in one step, which was further used for the electrode modification. A carbon ionic liquid (IL) electrode (CILE) was used as the substrate electrode due to its excellent performances such as wide potential range, certain electrocatalytic activity and good anti-fouling ability (Sun et al., 2007; Shiddiky and Torriero, 2011). Myoglobin (Mb) was used as the model for the investigation and the electrochemical behaviors of Mb on GR–SnO_2/CILE were investigated carefully. Nitrite is a commonly used chemical in industrial processes and food preservative, which can be found in water, food and physiological systems (Swann, 1975). It has been reported that nitrite can interact with amines to from carcinogenic nitrosamines (Mirvish, 1995). Therefore it is necessary to establish sensitive and selective methods for the quantitative determination of nitrite. Electrochemical biosensor with redox proteins has been used to catalyze the reductive reaction of nitrite and the results can be applied to the electrochemical sensor for the reduction of nitrite (Yang et al., 2005; Wei et al., 2009). Therefore the electrocatalytic ability of fabricated electrochemical sensor to the reduction of nitrite was carefully investigated. The fabricated electrochemical sensor exhibited good electrocatalytic activity for the successful construction of a third-generation electrochemical enzyme electrode without mediators.

2. Experimental

2.1. Reagents

1-Butylpyridinium hexafluorophosphate ($BPPF_6$, $\geqslant$99%, Lanzhou Greenchem. ILS. LICP. CAS., China), horseheart myoglobin (Mb, Sigma, MW = 17,800), graphite powder (average particle size 30 μm, Shanghai Colloid Chemical Plant, China) and Nafion (5% ethanol solution, Sigma) were used as received. 0.1 mol L^{-1} phosphate buffer solutions (PBS) with various pH values were used as the supporting electrolyte. All the other chemicals used were of analytical reagent grade and doubly distilled water was used in the experiments.

2.2. Apparatus

A CHI 750B electrochemical workstation (Shanghai CH Instrument, China) was used for all the electrochemical measurements. A conventional three-electrode system was used with an Mb-modified electrode as the working electrode, a platinum wire as the auxiliary electrode and a saturated

Please cite this article in press as: Wang, W. et al., Electrochemistry of myoglobin on graphene–SnO_2 nanocomposite modified electrode and its electrocatalysis. Arabian Journal of Chemistry (2015), http://dx.doi.org/10.1016/j.arabjc.2015.09.007

calomel electrode (SCE) as the reference electrode. Ultraviolet–visible (UV–Vis) absorption spectra and Fourier transform infrared (FT-IR) spectra were recorded on a Cary 50 probe spectrophotometer (Varian Company, Australia) and a Tensor 27 FT-IR spectrophotometer (Bruker Company, Germany), respectively. Transmission electron microscopy (TEM) was performed on an FEI Tecnai G2 F20 transmission electron microscope (FEI Company, USA) and scanning electron microscopy (SEM) was recorded on a JSM-7100F scanning electron microscope (JEOL Inc., Japan).

2.3. Preparation of the GR–SnO_2 nanocomposite

GR was synthesized by a solvothermal method reported in our previous work (Zhu et al., 2013). Briefly, 3.0 mL of tetrachloromethane was reacted with 4.0 g of potassium in an autoclave at 200 °C for 15 h. When the autoclave cooled down to room temperature after the reaction, the product was transferred to a beaker, and washed subsequently by HCl solution, de-ionized water, acetone, and de-ionized water, until the pH value of the solution reached to 7. Then the product was dried at 100 °C for 12 h.

For the synthesis of GR-supported SnO_2 nanoparticles (Dong et al., 2012), 192 mg of $SnCl_2{\cdot}2H_2O$ and 331 μL of HCl (38%) were dispersed in 60 mL of deionized water. Then 30 mg of GR was added into the solution, and the mixed solution was sonicated for 5 min and stirred for 30 min. Finally, the mixed solution was filtered, washed and dried in an oven at 70 °C for 12 h.

2.4. Preparation of the modified electrodes

Based on the reported procedure (Sun et al., 2007), CILE was fabricated by mixing 1.6 g of graphite powder and 0.8 g of $BPPF_6$ thoroughly in a mortar, which was filled into one end of a glass tube (Φ = 4.2 mm) with a copper wire inserted through the opposite end to establish an electrical contact. Prior to use a mirror-like surface was obtained by polishing the electrode on a weighing paper.

A mixture solution containing 12.0 mg mL^{-1} Mb and 0.5 mg mL^{-1} GR–SnO_2 nanocomposite was prepared and mixed homogeneously to obtain a suspension solution, and then 7.0 μL of the mixture was pipetted onto the surface of CILE and dried to get the modified electrode. Finally, 3.0 μL of 0.5% Nafion ethanol solution was cast on the electrode surface and dried to get a uniform film modified electrode, which was denoted as Nafion/Mb–GR–SnO_2/CILE and kept in refrigerator at 4 °C.

2.5. Procedure

Electrochemical measurements were carried out in a 10 mL electrochemical cell containing 0.1 mol L^{-1} PBS as the supporting electrolyte, which was purged with highly purified nitrogen for 30 min prior to the experiments and maintained in a nitrogen atmosphere during the experiments. UV–Vis absorption spectroscopic experiments were performed using a mixture solution containing certain concentrations of Mb and GR–SnO_2 nanocomposite, which was scanned in the wavelength range from 300 to 600 nm. The Mb–GR–SnO_2 film was assembled on a glass slide and air-dried to generate the composite, which was stripped off and tableted with KBr powder for the FT-IR experiments. For TEM characterizations, GR–SnO_2 nanocomposite was dispersed in an ethanol solution and ultrasonicated for 5 min. Several drops of suspension were then transferred onto a holey carbon TEM grid.

3. Results and discussion

3.1. Characteristics of GR–SnO_2 nanocomposite

The synthesis of GR–SnO_2 nanocomposite was similar to our former reported procedure (Dong et al., 2012). The morphology and structure of GR-supported SnO_2 nanoparticles were examined on an FEI Tecnai G2 F20 transmission electron microscope. Due to their low contrast under electron beam and small size of SnO_2 nanoparticles, it is challenging to show their distribution on GR surface at low magnifications. As given in Fig. 1A, GR sheet wrinkled together to reduce surface energy, and the dimension of GR sheets was smaller than 100 nm. High resolution TEM (HRTEM) image of GR–SnO_2 was presented in Fig. 1B. It was observed that SnO_2 nanoparticles with a dimension of 2–4 nm were uniformly formed on GR sheets. The tetragonal (1 1 0) and (1 0 1) planes with lattice spacing of 0.34 and 0.26 nm were marked in Fig. 1B, respectively. HRTEM characterizations reveal the formation and distribution of SnO_2 nanoparticles on the surface of GR. The resulted GR–SnO_2 nanocomposite still remains graphene-like nanosheet with large surface area, which is beneficial for its further interaction with Mb molecules. SEM image of GR–SnO_2 nanocomposite on the electrode surface was recorded and shown in Fig. 1C. It can be seen that the flake like GR sheets were present on the electrode surface, which was interconnected and associated with each other to give a porous structure. Therefore the effective surface area was increased greatly on the GR–SnO_2 modified electrode.

3.2. Spectroscopic results

UV–Vis absorption spectroscopy is an effective method to probe the structural change of heme proteins. The location of the Soret absorption band from the four iron heme groups of proteins can provide structural information about possible denaturation of heme proteins, especially the possible denaturation or the conformational change in the heme group region (George and Hanania, 1953). As shown in Fig. 2A, the Soret band of Mb dissolved in water appeared at 410.2 nm (curve a), while the similar Soret band appeared at 410.6 nm for a Mb–GR–SnO_2 mixture suspension solution in pH 5.0 PBS (curve b). The similar values indicated that Mb was not denatured after mixing with GR–SnO_2 nanocomposite.

FT-IR spectroscopy is usually used to provide detailed information on the secondary structure of polypeptide chains and to detect conformational changes of proteins. It is well-known that the amide I band at 1700–1600 cm^{-1} is caused by C═O stretching vibrations of the peptide linkage and the amide II band at 1600–1500 cm^{-1} results from a combination of N═H in-plane bending and C═N stretching of the peptide groups. If Mb molecule is denatured, the intensity and shape of the amide I and II bands would diminish or disappear (Song et al., 1992). From Fig. 2B, it can be seen that the amide I and II bands of native state of Mb appeared at 1656.44 cm^{-1}

Please cite this article in press as: Wang, W. et al., Electrochemistry of myoglobin on graphene–SnO_2 nanocomposite modified electrode and its electrocatalysis. Arabian Journal of Chemistry (2015), http://dx.doi.org/10.1016/j.arabjc.2015.09.007

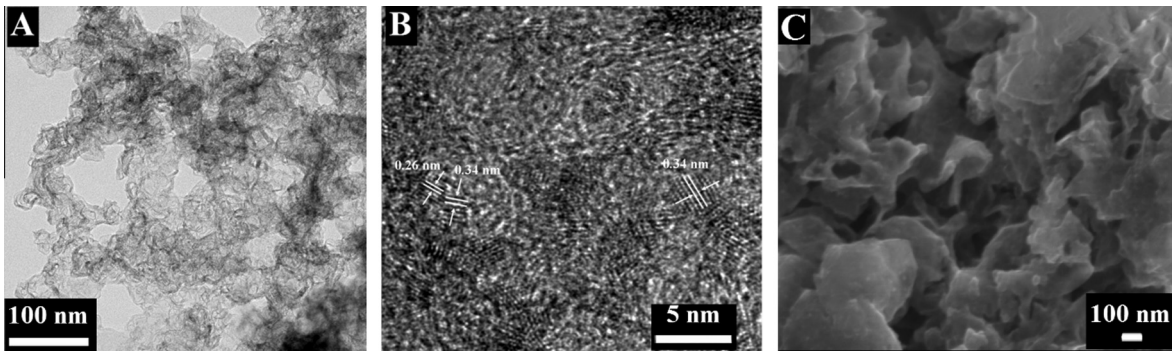

Figure 1 (A) TEM and (B) HRTEM images of GR–SnO_2 nanocomposite, (C) SEM image of GR–SnO_2/CILE.

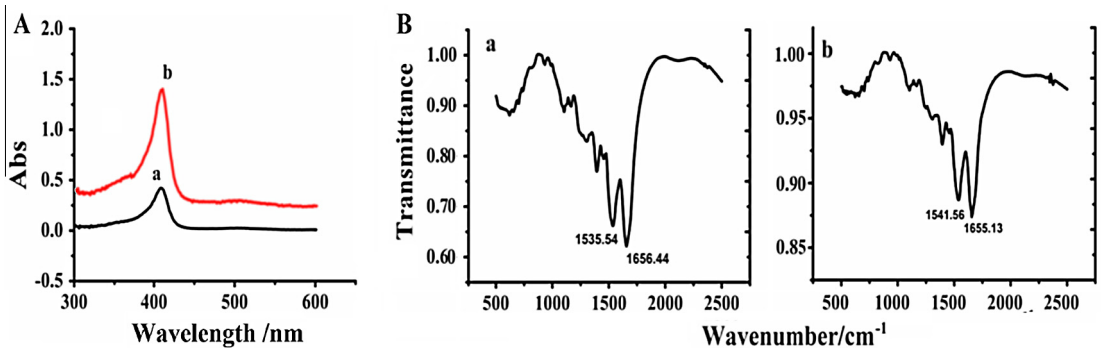

Figure 2 (A) UV–Vis absorption spectra of Mb in water (a) and Mb–GR–SnO_2 suspension in PBS (b); (B) FT-IR spectra of Mb (a) and Mb–GR–SnO_2 (b).

and 1535.54 cm^{-1} (Fig. 2Ba), and that of Mb in GR–SnO_2 film located at 1655.13 cm^{-1} and 1541.56 cm^{-1} (Fig. 2Bb). The similar positions of amide band suggested that Mb molecules still retained their native states after mixing with GR–SnO_2 nanocomposite.

3.3. EIS of the modified electrodes

EIS is a useful tool to investigate the impedance information of the electrode surface during the modification process. Fig. 3

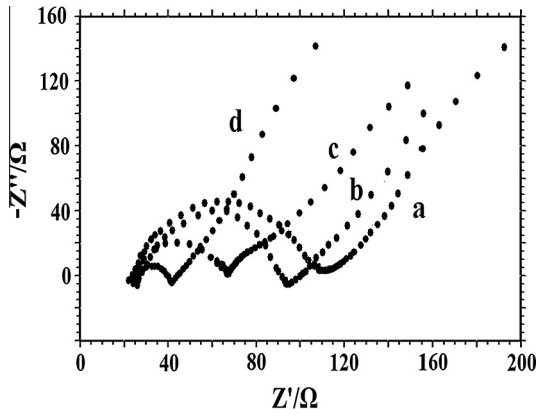

Figure 3 EIS for (a) Nafion/Mb–GR–SnO_2/CILE, (b) Nafion/GR–SnO_2/CILE, (c) CILE, and (d) GR–SnO_2/CILE in the solution of 10.0 mmol L^{-1} $[Fe(CN)_6]^{3-/4-}$ and 0.1 mol L^{-1} KCl with the frequencies swept from 10^4 to 0.1 Hz.

presented the Nyquist diagrams of different electrodes in a 10.0 mmol L^{-1} $[Fe(CN)_6]^{3-/4-}$ solution containing 0.1 mol L^{-1} KCl across the frequency range from 10^4 to 0.1 Hz. The semicircle diameter observed at higher frequency range equals to electron transfer resistance (R_{et}), which can imply the electron transfer kinetics of the redox probe at the electrode. As for CILE the R_{et} value was around 43.65 Ω (curve c), which can be ascribed to the presence of high conductive IL in the carbon paste. After the addition of GR–SnO_2 nanocomposite onto the CILE surface, the R_{et} value of GR–SnO_2/CILE decreased to 20.58 Ω (curve d). The result indicated that GR–SnO_2 nanocomposite exhibited good conductivity and decreased the interfacial resistance. On Nafion/GR–SnO_2/CILE the R_{et} value was increased to 75.89 Ω (curve b), which was due to the presence of Nafion film on the electrode surface that hindered the electron transfer of $[Fe(CN)_6]^{3-/4-}$. After Mb was immobilized in the film, the R_{et} value was further increased to 93.26 Ω (curve a), which indicated that the successful immobilization of Mb on the electrode surface further hindered the electron transfer and increased the resistance.

3.4. Cyclic voltammetric behavior of the Mb modified electrode

Cyclic voltammograms of different modified electrodes were recorded in a 0.1 mol L^{-1} PBS (pH 5.0) at a scan rate of 100 mV s^{-1}. As shown in Fig. 4, no redox peaks appeared on CILE (curve a) and Nafion/GR–SnO_2/CILE (curve b) but with the increase of background current. At Nafion/Mb/CILE a pair of unsymmetrical redox peaks were observed with

Please cite this article in press as: Wang, W. et al., Electrochemistry of myoglobin on graphene–SnO_2 nanocomposite modified electrode and its electrocatalysis. Arabian Journal of Chemistry (2015), http://dx.doi.org/10.1016/j.arabjc.2015.09.007

a cathodic peak (E_{pc}) at −0.303 V and an anodic peak (E_{pa}) at −0.226 V (curve c). CILE has been proven to be an excellent working electrode with many advantages, which can be used for the realization of direct electron transfer of redox proteins (Sun et al., 2007). On Nafion/Mb–GR–SnO_2/CILE a pair of well-defined and nearly symmetric redox peaks were observed with the redox peak currents increased obviously (curve d). The cathodic and anodic peak potentials were located at −0.318 V (E_{pc}) and −0.236 V (E_{pa}), respectively. The formal peak potential ($E^{0'}$), which was defined as the average value of E_{pc} and E_{pa}, was got as −0.272 V with a peak-to-peak separation (ΔE_p) of 82 mV. So the direct electron transfer of Mb was accelerated on the GR–SnO_2 modified CILE. The GR–SnO_2 nanocomposite exhibited as nanosheets with SnO_2 nanoparticles dispersed on the surface of GR, which showed synergistic effects, including the high conductivity and large surface area of GR and the biocompatibility of SnO_2 nanoparticles. Therefore direct electrochemistry of Mb was accelerated on the GR–SnO_2 modified electrode with a pair of well-defined redox peaks appeared.

3.5. Electrochemical behaviors

Cyclic voltammograms of Nafion/Mb–GR–SnO_2/CILE in 0.1 mol L^{-1} PBS at different scan rates were further investigated from 30 to 500 mV s^{-1} with the results shown in Fig. 5A. It can be seen that a pair of well-defined quasi-reversible redox peaks appeared at different scan rates with almost equal value of peak currents. The relationship of the electrochemical data with scan rate was further calculated. The linear regression equations of redox peak currents with scan rate were calculated as $I_{pc}(\mu A) = 227.33\upsilon$ (V s^{-1}) + 9.52 (n = 12, γ = 0.996) and $I_{pa}(\mu A) = -232.14\upsilon$ (V s^{-1}) −2.46 (n = 12, γ = 0.996), respectively (as shown in Fig. 5B), which indicated an adsorption-controlled electrochemical process. Based on the equation of $\Gamma^* = Q/nAF$ (Bard and Faulkner, 1980), the surface concentration (Γ^*) of electroactive Mb was calculated to be 1.3×10^{-9} mol cm^{-2}. The total amount of Mb cast on the electrode surface was 4.72×10^{-9} mol cm^{-2}, therefore 27.5% of the Mb molecules on the electrode surface participated in the electrochemical reaction. So the presence of GR–SnO_2 nanocomposite exhibited a larger surface area that was efficient for Mb immobilization, which could provide a specific conductive interface for multiple layers of Mb near the electrode surface to transfer electrons with the basal electrode.

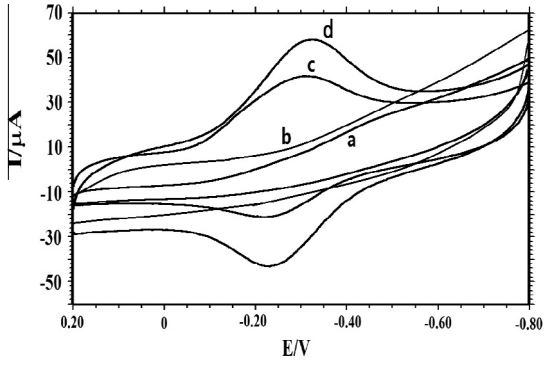

Figure 4 Cyclic voltammograms of (a) CILE, (b) Nafion/GR–SnO_2/CILE, (c) Nafion/Mb/CILE, and (d) Nafion/Mb–GR–SnO_2/CILE in pH 5.0 PBS with the scan rate as 100 mV s^{-1}.

From Fig. 5A it can be seen that with the increase of scan rate the redox peak potential shifted slightly with ΔE_p value increased gradually. Two straight lines were obtained with the equations of E_{pc}(V) = −0.026 lnυ −0.37 (γ = 0.995) and E_{pa}(V) = 0.28 lnυ −0.19 (γ = 0.997), respectively. According to the Laviron's equation (Laviron, 1974; Laviron, 1979), the values of the electron transfer coefficient (α) and the heterogeneous electron transfer rate constant (k_s) were calculated as 0.519 and 1.034 s^{-1}, respectively. It is well known that k_s value reflects the local microenvironment of protein immobilized on the electrode. This k_s value is higher than the values of Mb when immobilized on C_{60}-multiwalled CNT based electrode (0.39 s^{-1}, Zhang et al., 2006), Ag–CNTs modified GCE (0.41 s^{-1}, Liu and Hu, 2009), NiO nanoparticle modified GCE (0.34 s^{-1}, Moghaddam et al., 2008), Co nanoparticle modified CILE (0.588 s^{-1}, Sun et al., 2009) and GO–IL modified CILE (0.584 s^{-1}, Sun et al., 2013), indicating the electron transfer of Mb was facilitated on GR–SnO_2 nanocomposite modified electrode.

In most cases the redox behavior of protein is significantly dependent on the solution pH, therefore the influence of buffer pH from 2.0 to 8.0 on cyclic voltammetric behaviors of Nafion/Mb–GR–SnO_2/CILE was investigated in 0.1 mol L^{-1} PBS with the results shown in Fig. 6. Nearly reversible voltammograms with stable and well-defined redox peaks were observed and the maximum redox peak current was occurred at pH 5.0, which was selected for the electrochemical investigation. Furthermore, negative shifts in both cathodic and anodic peak potentials were observed with increasing pH value, indicating that protons took part in the electrode reaction. The formal peak potential ($E^{0'}$) had a linear relationship with the buffer pH and the regression equation was calculated as $E^{0'}$(mV) = −48.1 pH +13.5 (γ = 0.998). The slope of −48.1 mV pH^{-1} was smaller than the theoretical value of −59.0 mV pH^{-1} for a one-electron one-proton reaction between the electrode and Mb. The reason might be the influence of the protonation states of transligands to the heme iron and amino acids around the heme or the protonation of the water molecule coordinated with the central iron. So the electrochemical reaction can be expressed with the equation as: Mb Fe(III) + H^+ + e → Mb Fe(II), which involved a single protonation accompanied with one electron transfer of Mb Fe(III) to electrode.

3.6. Electrocatalytic behaviors of the immobilized Mb

The Mb immobilized on the electrode surface exhibited excellent electrocatalytic ability to the reduction of $NaNO_2$. Fig. 7A shows the cyclic voltammograms of Nafion/Mb–GR–SnO_2/CILE in PBS containing different concentrations of $NaNO_2$ at a fixed scan rate of 100 mV s^{-1}. Upon the addition of $NaNO_2$, a new irreversible reduction peak appeared at −0.812 V, which was attributed to the reduction of NO_2^- by Mb molecules on the electrode. While on Nafion/GR–SnO_2/CILE the direct electrochemical reduction of nitrite required a large potential with the reduction peak potential appeared −0.998 V (Fig. 7B curves i and j) without the appearance of the oxidation peak. The overpotential of electroreduction of

Please cite this article in press as: Wang, W. et al., Electrochemistry of myoglobin on graphene–SnO_2 nanocomposite modified electrode and its electrocatalysis. Arabian Journal of Chemistry (2015), http://dx.doi.org/10.1016/j.arabjc.2015.09.007

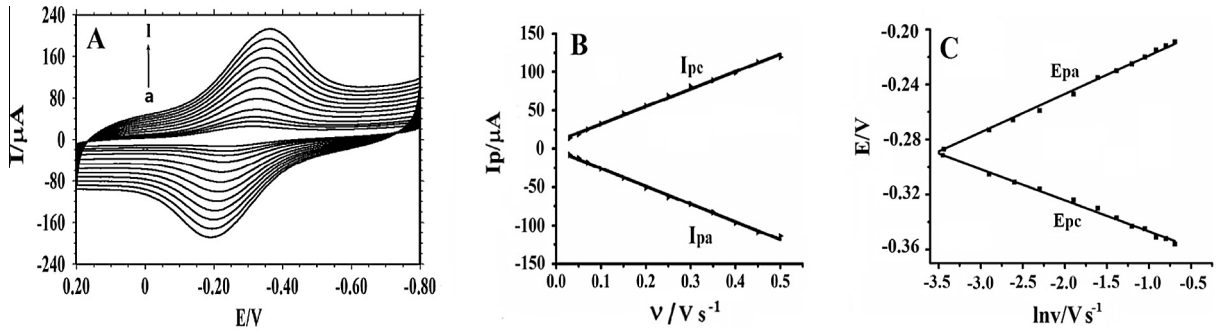

Figure 5 (A) Influence of scan rate on electrochemical responses of Nafion/Mb–GR–SnO_2/CILE in pH 5.0 PBS with scan rates from (a) to (l) as 30, 50, 70, 100, 150, 200, 250, 300, 350, 400, 450, 500 mV s^{-1}, respectively. (B) Linear relationship of redox peak current (Ip) versus scan rate (υ). (C) Linear relationship of the redox potential versus ln υ.

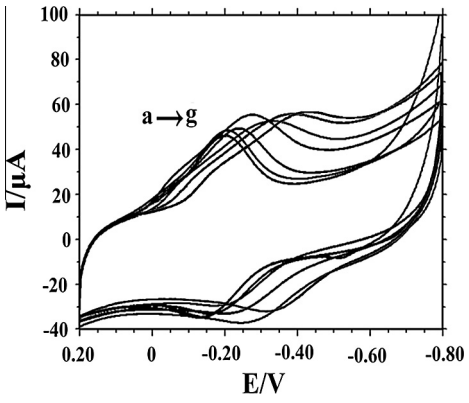

Figure 6 Cyclic voltammograms of Nafion/Mb–GR–SnO_2/CILE in different pH PBS (from a to g as 2, 3, 4, 5, 6, 7, 8) with the scan rate of 100 mV s^{-1}.

nitrite was lower for 0.186 V. Therefore the presence of Mb molecules on the electrode exhibited the catalytic behaviors with the decrease of the activation energy for the reaction and the increase of the reduction peak current. Based on the references (Yomathan et al., 1992; Shan et al., 2005), the reaction process can be proposed as follows:

$$\text{Mb Fe(III)} + H^+ + e^- \rightarrow \text{Mb Fe(II)} \quad \text{at electrode} \tag{1}$$

$$NO_2^- + H^+ \rightleftharpoons HNO_2 \tag{2}$$

$$3HNO_2 \rightarrow 2NO + NO_3^- + H^+ + H_2O \tag{3}$$

$$NO + \text{Mb Fe(II)} \rightarrow \text{Mb Fe(II)} - NO \tag{4}$$

$$\text{Mb Fe(II)—NO} + H^+ + e^- \rightarrow \text{Mb Fe(II)} + \text{product} + H_2O \quad \text{at electrode} \tag{5}$$

This reaction mechanism indicates that nitrite combines with a proton to get HNO_2 firstly, which is disproportionated to NO and NO_3^- subsequently. Then Mb Fe(II) formed on the electrode surface reacts with NO to get the ferrous nitrosyl complex of Mb Fe(II)—NO, which can directly reduce on the electrode surface to release Mb Fe(II) again with a catalytic cycle formed.

The reduction peak current increased along with $NaNO_2$ concentration in the range from 0.2 to 350.0 μmol L^{-1} with the linear regression equation got as I_{ss}(μA) = 8.901 + 29.77C (μmol L^{-1}) and the detection limit of 0.483 μmol L^{-1} (S/N = 3). When the concentration of $NaNO_2$ was more than 400.0 μmol L^{-1}, a current plateau appeared, which was the typical Michaelis–Menten process. For a thin film of immobilized proteins, the maximum current measured under the saturated substrate conditions (I_{max}) and the apparent Michaelis–Menten constant (K_M^{app}), which give an indication of the enzyme-substrate kinetics, can be obtained from the Lineweaver–Burk equation (Kamin and Willson, 1980):

$$\frac{1}{I_{SS}} = \frac{1}{I_{max}} + \frac{K_{app}^M}{I_{max}C}$$

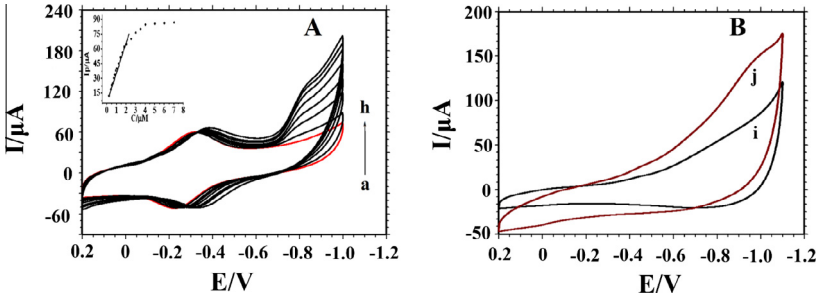

Figure 7 Cyclic voltammograms of (A) Nafion/Mb–SnO_2–GR/CILE in 0.1 mol L^{-1} pH 5.0 PBS with different concentrations of $NaNO_2$ (From a to h: 0, 2.0, 5.0, 7.0, 9.0, 14.0, 18.0, 20.0 μmol L^{-1}) at the scan rate of 100 mV s^{-1}. Inset is linear relationship of catalytic reduction peak currents versus the $NaNO_2$ concentration; (B) Nafion/SnO_2–GR/CILE in 0.1 mol L^{-1} pH 5.0 PBS with 0 and 2.50 mmol L^{-1} $NaNO_2$ (From i to j) at the scan rate of 100 mV s^{-1}.

Table 1 Comparisons of different protein modified electrodes for electrochemical detection of nitrite.

Modified electrodes	Method	Linear range (μmol L^{-1})	Detection limit (μmol L^{-1})	Refs.
CytC/Cu–LDH/Nafion/Au	Amperometry	0.75–123.0	0.2	Yin et al. (2010)
Mb–ZnO/GCE	Amperometry	10–180	4.0	Zhao et al. (2006)
Hb/RTILs/MWCNTs/GCE	Amperometry	4–320	0.81	Wei et al. (2009)
SiO_2/Cyts/SiO_2/BDD	Amperometry	1–1000	0.5	Geng et al. (2008)
Hb/HS–CdS/GCE	Amperometry	0.3–182	0.08	Dai et al. (2008)
CTS–Hb–CNT–IL/CILE	Voltammetry	400–8000	100	Zhu et al. (2010)
SA–Mb–IL–Fe_3O_4/CILE	Voltammetry	4.0×10^3–1.0×10^5	1.3×10^3	Zhan et al. (2010)
Nafion/Mb–Co_3O_4–Au/CILE	Voltammetry	40.0–260.0	10	Wang et al. (2014)
Hb/PI/COOH–MWCNT/GCE	Amperometry	3–68	0.63	Kou et al. (2012)
Hb/Ag/TiO_2/GCE	Amperometry	4.0–350.0	1.2	Yang et al. (2005)
Nafion/Mb–GR–SnO_2/CILE	Voltammetry	0.2–350.0	0.483	This work

Table 2 Determination of nitrite in different water samples.

Sample	Content (μmol L^{-1})	Added (μmol L^{-1})	Found (μmol L^{-1})	RSD (%)	Recovery (%)
Tap water	0	100.0	99.5	1.78	99.5
	0	200.0	202.2	3.01	101.1
	0	300.0	307.8	3.73	102.6
Lake water	0	100.0	103.1	2.54	103.1
	0	200.0	202.6	1.86	101.3
	0	300.0	297.8	3.34	99.3

where C is the bulk concentration of the substrate. Based on the above equation the K_M^{app} value for this $NaNO_2$ biosensor was calculated to be 3.98 μmol L^{-1}. A comparison of the proposed bioelectrode for the electrocatalytic detection of $NaNO_2$ with other redox protein modified electrodes was summarized and listed in Table 1. It can be seen that this electrode showed excellent electrochemical behaviors with wider linear range and lower detection limit, indicated the specific characteristic of GR–SnO_2 nanocomposite for the efficiency electron transfer of Mb molecules with electrode.

3.7. Stability and reproducibility of Nafion/Mb–GR–SnO_2/CILE

The stability of Nafion/Mb–GR–SnO_2/CILE was also investigated. Firstly the modified electrode was evaluated by examining the cyclic voltammetric peak currents after continuous scanning for 50 cycles. There was nearly no decrease of the voltammetric response and 99.1% of the initial current response was retained. After the modified electrode was stored in a refrigerator at 4 °C for two weeks, 5.5% decrease of the peak current appeared. After a 30-day storage, Nafion/Mb–GR–SnO_2/CILE still retained 91.2% of its initial current response. The relatively good stability of the Mb electrode could be attributed to the biocompatibility of the GR–SnO_2 nanomaterial in the film. Six Mb modified electrodes prepared by the same procedure gave the relative standard deviation (RSD) of 3.2% for the determination of 10.0 μmol L^{-1} $NaNO_2$ solution, which indicated the modified electrode had good repeatability.

3.8. Sample determination

To evaluate the possible application of the proposed electrode for the real samples detection, different water samples including tap water and lake water were tested, which were diluted with pH 5.0 PBS and detected by the recommended procedure. All the samples were further measured by the standard addition method to calculate the recovery with the results summarized in Table 2. It can be seen that the recovery of this method was in the range from 99.3% to 103.1%, which was satisfied for the routine analysis.

4. Conclusion

In this paper a GR–SnO_2 nanocomposite was synthesized and used to construct a redox protein-based electrochemical sensor, which exhibited good biocompatibility and provided specific microenvironments for the immobilization of Mb molecules. Direct electron transfer process of Mb was enhanced on the modified electrode with the electrochemical parameters calculated. The Mb and GR–SnO_2 nanocomposite modified electrode exhibited an excellent enzyme-like catalytic activity for the reduction of $NaNO_2$. Thus the GR–SnO_2 nanocomposite can act as an effective support matrix for protein immobilization and the modified electrodes could provide a new platform to fabricate the third-generation biosensors based on the direct electrochemistry of redox protein.

Acknowledgments

This project was partially supported by the Taishan Overseas Scholar program (tshw20091005), the International Science & Technology Cooperation Program of China (2014DFA60150), the National Natural Science Foundation of China (51172113, 21365010), the Natural Science Foundation of Hainan Province (20152016), the International Science & Technology Cooperation Project of Hainan Province (KJHZ2015-13) and the Natural Science Foundation of Shandong Province (JQ201118).

References

Armstrong, F.A., Hill, H.A.O., Walton, N.J., 1988. Direct electrochemistry of redox proteins. Acc. Chem. Res. 21, 407–413.
Bard, A.J., Faulkner, L.R., 1980. Electrochemical Methods: Fundamentals and Applications. Wiley, New York.
Brownson, D.A.C., Kampouris, D.K., Banks, C.E., 2012. Graphene electrochemistry: fundamental concepts through to prominent applications. Chem. Soc. Rev. 41, 6944–6976.
Chen, D., Tang, L.H., Li, J.H., 2010. Graphene-based materials in electrochemistry. Chem. Soc. Rev. 39, 3157–3180.
Dai, Z., Bai, H., Hong, M., Zhu, Y., Bao, J., Shen, J., 2008. A novel nitrite biosensor based on the direct electron transfer of hemoglobin immobilized on CdS hollow nanospheres. Biosens. Bioelectron. 23, 1869–1873.
Ding, S.J., Luan, D.Y., Boey, F.Y.C., Chen, J.S., Lou, X.W., 2011. SnO_2 nanosheets grown on graphene sheets with enhanced lithium storage properties. Chem. Commun. 47, 7155–7157.
Dong, L.F., Hansen, J., Xu, P., Ackerman, M.L., Barber, S.D., Schoelz, J.K., Qi, D., Thibado, P.M., 2012. Electromechanical properties of freestanding graphene functionalized with tin oxide (SnO_2) nanoparticles. Appl. Phys. Lett. 101, 061601.
Gan, T., Hu, S.S., 2011. Electrochemical sensors based on graphene materials. Microchim. Acta 175, 1–19.
Geim, A.K., Novoselov, K.S., 2007. The rise of graphene. Nat. Mater. 6, 183–191.
Geng, R., Zhao, G., Liu, M., Li, M., 2008. A sandwich structured SiO_2/cytochrome c/SiO_2 on a boron-doped diamond film electrode as an electrochemical nitrite biosensor. Biomaterials 29, 2794–2801.
George, P., Hanania, C., 1953. A spectrophotometric study of ionizations in methaemoglobin. Biochem. J. 55, 236–243.
Gorton, L., Lindgren, A., Larsson, T., Munteanu, F.D., Ruzgas, T., Gazaryan, I., 1999. Direct electron transfer between heme-containing enzymes and electrodes as basis for third generation biosensors. Anal. Chim. Acta 400, 91–108.
Huang, X.D., Zhou, X.F., Zhou, L., Qian, K., Wang, Y.H., Liu, Z.P., Yu, C.I., 2011. A facile one-step solvothermal synthesis of SnO_2/-graphene nanocomposite and its application as an anode material for lithium-ion batteries. ChemPhysChem 12, 278–281.
Idota, Y., Kubota, T., Matsufuji, A., Maekawa, Y., Miyasaka, T., 1997. Tin-based amorphous oxide: a high-capacity lithium-lon-storage material. Science 276, 1395–1397.
Kamin, R.A., Willson, G.S., 1980. Rotating ring-disk enzyme electrode for biocatalysis kinetic studies and characterization of the immobilized enzyme layer. Anal. Chem. 52, 1198–1205.
Kou, H.H., Jia, L.P., Wang, C.M., Ye, W.C., 2012. A nitrite biosensor based on the direct electron transfer of hemoglobin immobilized on carboxyl-functionalized multiwalled carbon nanotubes/polyimide composite. Electroanalysis 24, 1799–1803.
Krishnakumar, T., Pinna, N.K., Kumari, P., Perumal, K., Jayaprakash, R., 2008. Microwave-assisted synthesis and characterization of tin oxide nanoparticles. Mater. Lett. 62, 3437–3440.
Laviron, E., 1974. Adsorption, autoinhibition and autocatalysis in polarography and in linear potential sweep voltammetry. J. Electroanal. Chem. 52, 355–359.
Laviron, E., 1979. General expression of the linear potential sweep voltammogram in the case of diffusionless electrochemical systems. J. Electroanal. Chem. 101, 19–28.
Li, D., Müller, M.B., Gilje, S., Kaner, R.B., Wallace, G.G., 2008. Processable aqueous dispersions of graphene nanosheets. Nat. Nanotechnol. 3, 101–105.
Li, Y.M., Lv, X.J., Lu, J., Li, J.H., 2010. Preparation of SnO_2-nanocrystal/graphene-nanosheets composites and their lithium storage ability. J. Phys. Chem. C 114, 21770–21774.
Lian, P.C., Wang, J., Cai, D.D., Ding, L.X., Jia, Q.M., Wang, H.H., 2014. Porous SnO_2@C/graphene nanocomposite with 3D carbon conductive network as a superior anode material for lithium-ion batteries. Electrochim. Acta 116, 103–110.
Liu, C.Y., Hu, J.M., 2009. Hydrogen peroxide biosensor based on the direct electrochemistry of myoglobin immobilized on silver nanoparticles doped carbon nanotubes film. Biosensors Bioelectron. 24, 2149–2154.
Lu, T., Zhang, Y.P., Li, H.B., Pan, L.K., Li, Y.L., Sun, Z., 2010. Electrochemical behaviors of graphene–ZnO and graphene–SnO_2 composite films for supercapacitors. Electrochim. Acta 55, 4170–4173.
Mani, V., Devadas, B., Chen, S.M., Li, Y., 2012. Immobilization of enzymes and redox proteins and their electrochemical biosensor applications. ECS Trans. 50, 35–41.
Mirvish, S.S., 1995. Role of N-nitroso compounds (NOC) and N-nitrosation in etiology of gastric, esophageal, nasopharyngeal and bladder cancer and contribution to cancer of known exposures to NOC. Cancer Lett. 93, 17–48.
Moghaddam, A.B., Ganjali, M.R., Dinarvand, R., Ahadi, S., Saboury, A.A., 2008. Myoglobin immobilization on electrodeposited nanometer-scale nickel oxide particles and direct voltammetry. Biophys. Chem. 134, 25–33.
Pumera, M., 2010. Graphene-based nanomaterials and their electrochemistry. Chem. Soc. Rev. 39, 4146–4157.
Rusling, J.F., 1998. Enzyme bioelectrochemistry in cast biomembrane-like films. Acc. Chem. Res. 31, 363–369.
Sahm, T., Rong, W., Barsan, N., Madler, L., Weimar, U., 2007. Sensing of CH_4, CO and ethanol with in situ nanoparticle aerosol-fabricated multilayer sensors. Sensors Actuators B – Chem. 127, 63–68.
Shan, W.J., He, P.L., Hu, N.F., 2005. Substrates on hydrogel triblock copolymer Pluronic films containing hemoglobin or myoglobin based on protein direct electrochemistry. Electrochim. Acta 51, 432–440.
Shao, Y.Y., Wang, J., Wu, H., Liu, J., Aksay, I.A., Lin, Y.H., 2010. Graphene based electrochemical sensors and biosensors: a review. Electroanalysis 22, 1027–1036.
Shiddiky, J.A.M., Torriero, A.A.J., 2011. Application of ionic liquids in electrochemical sensing systems. Biosensors Bioelectron. 26, 1775–1787.
Singh, V., Joung, D., Zhai, L., Das, S., Khondaker, S.I., Seal, S., 2011. Graphene based materials: past, present and future. Prog. Mater Sci. 56, 1178–1271.
Song, Y.P., Petty, M.C., Yarwood, J., Feast, W.J., Tsibouklis, J., Mukherjee, S., 1992. Fourier transform infrared studies of molecular ordering and interactions in Langmuir–Blodgett films containing nitrostilbene and stearic acid. Langmuir 8, 257–261.
Sun, W., Gao, R.F., Jiao, K., 2007. Research and application of ionic liquids in analytical chemistry. Chin. J. Anal. Chem. 35, 1813–1819.
Sun, W., Yang, M.X., Jiao, K., 2007. Electrocatalytic oxidation of dopamine at an ionic liquid modified carbon paste electrode and its analytical application. Anal. Bioanal. Chem. 389, 1283–1291.
Sun, W., Wang, D.D., Gao, R.F., Jiao, K., 2007. Direct electrochemistry and electrocatalysis of hemoglobin in sodium alginate film on a $BMIMPF_6$ modified carbon paste electrode. Electrochem. Commun. 9, 1159–1164.
Sun, W., Li, X.Q., Qin, P., Jiao, K., 2009. Electrodeposition of Co nanoparticles on the carbon ionic liquid electrode as a platform for myoglobin electrochemical biosensor. J. Phys. Chem. C 113, 11294–11300.
Sun, W., Wang, X.Z., Wang, Y.H., Ju, X.M., Xu, L., Li, G.J., Sun, Z. F., 2013. Application of graphene–SnO_2 nanocomposite modified electrode for the sensitive electrochemical detection of dopamine. Electrochim. Acta 87, 317–322.
Sun, W., Li, L.F., Lei, B.X., Li, T.T., Ju, X.M., Wang, X.Z., Li, G.J., Sun, Z.F., 2013. Fabrication of graphene–platinum nanocomposite for the direct electrochemistry and electrocatalysis of myoglobin. Mater. Sci. Eng. C – Mater. Biol. Appl. 33, 1907–1913.

Please cite this article in press as: Wang, W. et al., Electrochemistry of myoglobin on graphene–SnO_2 nanocomposite modified electrode and its electrocatalysis. Arabian Journal of Chemistry (2015), http://dx.doi.org/10.1016/j.arabjc.2015.09.007

Swann, P.F., 1975. The toxicology of nitrate, nitrite and n-nitroso compounds. J. Sci. Food Agric. 26, 1761–1770.
Wang, J., 2006. Analytica Electrochemistry, third ed. John Wiley and Sons, Hoboken, New Jersey.
Wang, X.Y., Zhou, X.F., Yao, K., Zhang, J.G., Liu, Z.P., 2011. A SnO_2/graphene composite as a high stability electrode for lithium ion batteries. Carbon 49, 133–139.
Wang, H.B., Maiyalagan, T., Wang, X., 2012. Review on recent progress in nitrogen-doped graphene: synthesis, characterization, and its potential applications. ACS Catal. 2, 781–794.
Wang, X.F., You, Z., Sha, H.L., Gong, S.X., Niu, Q.J., Sun, W., 2014. Direct electrochemistry and electrocatalysis of myoglobin using an ionic liquid-modified carbon paste electrode coated with Co_3O_4 nanorods and gold nanoparticles. Microchim. Acta 181, 767–774.
Wei, W., Jin, H.H., Zhao, G.C., 2009. A reagentless nitrite biosensor based on direct electron transfer of hemoglobin on a room temperature ionic liquid/carbon nanotube-modified electrode. Microchim. Acta 164, 167–171.
Yang, X.H., Wang, L.L., 2007. Synthesis of novel hexagon SnO_2 nanosheets in ethanol/water solution by hydrothermal process. Mater. Lett. 61, 3705–3707.
Yang, W.W., Bai, Y., Li, Y.C., Sun, C.Q., 2005. Amperometric nitrite sensor based on hemoglobin/colloidal gold nanoparticles immobilized on a glassy carbon electrode by a titania sol–gel film. Anal. Bioanal. Chem. 382, 44–50.
Yao, J., Shen, X.P., Wang, B., Liu, H.K., Wang, G.X., 2009. In situ chemical synthesis of SnO_2–graphene nanocomposite as anode materials for lithium-ion batteries. Electrochem. Commun. 11, 1849–1852.
Yin, H.S., Zhou, Y.L., Liu, T., Cui, L., Ai, S.Y., Qiu, Y.Y., Zhu, L.S., 2010. Amperometric nitrite biosensor based on a gold electrode modified with cytochrome c on Nafion and Cu–Mg–Al layered double hydroxides. Microchim. Acta 171, 385–392.
Yomathan, J.N., Wood, K.S., Meyer, T.J., 1992. Electrocatalytic reduction of nitrite and nitrosyl by iron(III) protoporphyrin IX dimethyl ester immobilized in an electropolymerized film. Inorg. Chem. 31, 3280–3285.
Zhan, T.R., Xi, M.Y., Wang, Y., Sun, W., Hou, W.G., 2010. Direct electrochemistry and electrocatalysis of myoglobin immobilized on Fe_2O_3 nanoparticle–sodium alginate–ionic liquid composite-modified electrode. J. Colloid Interface Sci. 346, 188–193.
Zhang, H., Fan, L.Z., Yang, S.H., 2006. Significantly accelerated direct electron-transfer kinetics of hemoglobin in a C_{60}-MWCNT nanocomposite film. Chem. – Eur. J. 12, 7161–7166.
Zhao, G., Xu, J., Chen, H., 2006. Interfacing myoglobin to graphite electrode with an electrodeposited nanoporous ZnO film. Anal. Biochem. 350, 145–150.
Zhu, J.J., Lu, Z.H., Aruna, S.T., Aurbach, D., Gedanken, A., 2000. Sonochemical synthesis of SnO_2 nanoparticles and their preliminary study as Li insertion electrodes. Chem. Mater. 12, 2557–2566.
Zhu, Z.H., Qu, L.N., Li, X., Zeng, Y., Sun, W., Huang, X.T., 2010. Direct electrochemistry and electrocatalysis of hemoglobin with carbon nanotube-ionic liquid–chitosan composite materials modified carbon ionic liquid electrode. Electrochim. Acta 55, 5959–5965.
Zhu, Q.Q., Yu, J.H., Zhang, W.S., Dong, H.Z., Dong, L.F., 2013. Solvothermal synthesis of boron-doped graphene and nitrogen-doped graphene and their electrical properties. J. Renew. Sustain. Energy 5, 021408.

Please cite this article in press as: Wang, W. et al., Electrochemistry of myoglobin on graphene–SnO_2 nanocomposite modified electrode and its electrocatalysis. Arabian Journal of Chemistry (2015), http://dx.doi.org/10.1016/j.arabjc.2015.09.007